Progress In Electromagnetics Research C, Vol. 136, 87–99, 2023

High Gain Multiband Microstrip Antenna for LTE, WLAN, Amateur Radio, and Sub-6 GHz 5G Applications

Pradeep Reddy and Veeresh G. Kasabegoudar*

Abstract—This paper presents a novel gap coupled suspended multiband microstrip antenna suitable for wireless applications like long term evolution (LTE), wireless local area network (WLAN), Amateur radio, and Sub 6 GHz 5G wireless applications. The proposed antenna is a single layer geometry suspended in air that employs a gap-coupled feed with a parasitic strip for tuning the input impedance. The overall dimensions of the antenna are 41.4 mm × 39 mm × 3.12 mm. The presented antenna offers a total of six resonant frequencies centered at 1.70 GHz, 2.77 GHz, 3.03 GHz, 4.26 GHz, 4.58 GHz, and 5.64 GHz. Measured resonant frequencies fairly match the simulated values. Further, the gain values at these frequencies are 7.29 dBi, 6.10 dBi, 7.39 dBi, 5.39 dBi, 6.22 dBi, & 7.03 dBi, and the corresponding measured gain values are 6.92 dBi, 7.72 dBi, 4.88 dBi, 5.34 dBi, 4.25 dBi, and 6.51 dBi, respectively. Radiation patterns were measured at all these frequencies and found to have highly stable radiation characteristics except for slight asymmetry at the high frequency end of the operational band.

1. INTRODUCTION

Rapid growth in subscribers in wireless applications has posed many constraints to antenna researchers, such as the requirement of antennas capable of handling high data rates with wide and/or multi-band operations. In order to meet these requirements, numerous researchers have addressed and proposed several works [1–5]. However, modern wireless appliances focus on the integration of several applications into one device [6]. It is well known that microstrip multiband antennas are suitable candidates to fulfil these demands due to their inherent advantages.

There are numerous works available in the literature that address dual [7–11], triple [12–17], and multi-band microstrip antennas [18–25]. Although some of these works [14–18] claim multiband operations, they offer only three bands. On the other hand, the antennas presented in [21, 22] offer a total of five resonances but have poor gain values. Another work reported in [23] provides 6 resonant bands and uses eight switches for multibeam characteristics. This antenna has a complex design procedure and has poor gain at all resonances. Another work reported in [25] offers a maximum of seven resonant bands. However, this antenna also exhibits poor gain at all bands. From the literature review, it may be noted that some antennas are simple to design but offer either dual- or triple-band operation. On the other hand, multiband antennas have adopted complex design procedures. Further, many of these multiband antennas suffer from poor gain characteristics.

Hence, in this paper, an effort has been made to design and investigate a simple single layer multi-band antenna that excites six resonant bands with good gain and stable radiation parameters at each of these operational frequencies. Detailed parametric studies have been carried out to optimize the presented antenna and are covered in the subsequent sections of this paper.

Section 2 outlines the proposed antenna's main geometry and physical specifications. The proposed antennas with gap coupled feed were optimised after a thorough parametric research, as described in

Received 11 June 2023, Accepted 4 August 2023, Scheduled 14 August 2023
* Corresponding author: Veeresh G. Kasabegoudar (veereshgk2002@rediffmail.com).
The authors are with the ECE Department, School of Engineering, Central University of Karnataka, Kalaburagi, India.

Section 3. Section 4 presents experimental data and interpretation of the findings. The work done in this paper comes to a conclusion in Section 5.

2. PROPOSED BASIC GEOMETRY

The basic geometry of the proposed antenna consists of three parts viz., a rectangular ring, a rectangular patch with a slot, and a small tapered parasitic strip placed alongside the length of the rectangular patch element. The basic geometry with probe feed is shown in Figure 1. A coaxial probe is placed at the middle of the parasitic tapered strip. However, the probe pin is physically not connected to any of the antenna parts, i.e., gap coupling is used for feeding the antenna. A small tapered strip is used, as suggested in [9]. More details on designing the antenna can be found there. The basic geometry is derived from combining the geometries of [9] and [10] so that the proposed antenna excites six resonances as opposed to just two resonances in [9] and [10]. It may be noted that the use of a patch alone with a slot produces only two resonant frequencies [9]. Similarly, in [10], the use of two rings also produces only two resonant modes. Hence, the inner ring of [10] is replaced with a slotted rectangular patch as used in [10] to excite a total of six resonances. Further, the working and detailed design procedure of a gap-coupled suspended microstrip antenna can be found in the work reported earlier by this group [6]. The patch antenna dimensions are calculated from the traditional length and width expressions of a microstrip antenna. It may be noted that the total height must be taken as $(g+h)$, and while calculating

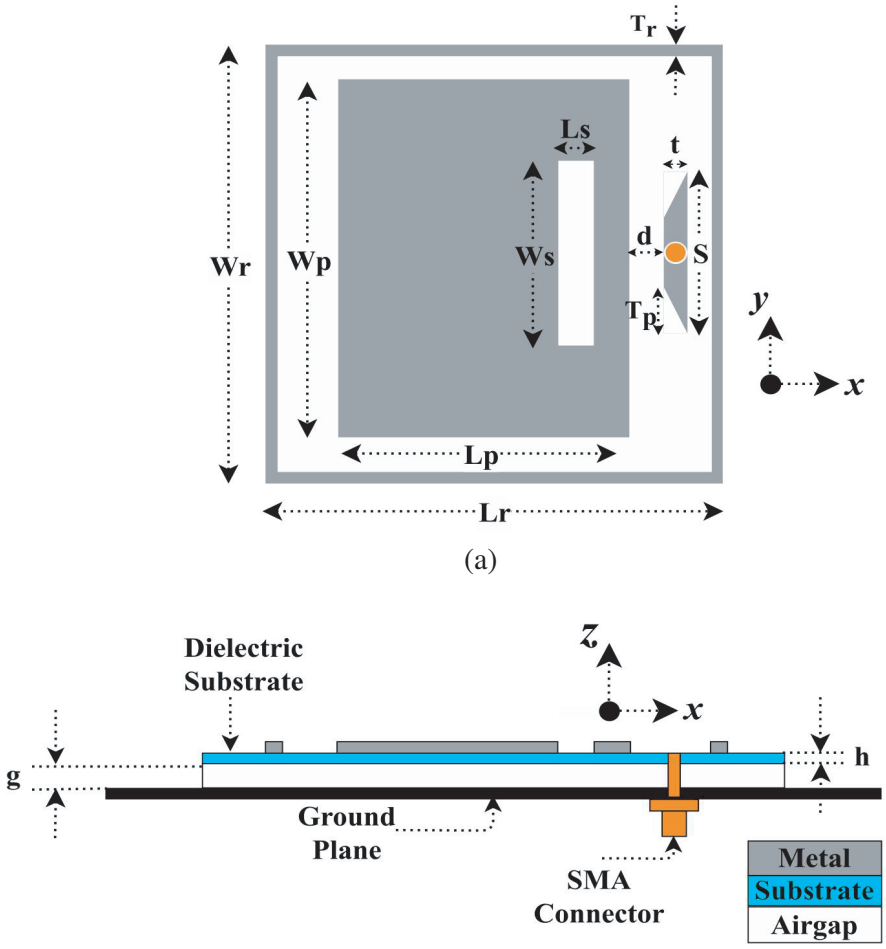

Figure 1. Suspended microstrip antenna with gap coupled probe feed. (a) Top view. (b) Cross sectional view.

the effective dielectric constant, the air-dielectric combination has to be taken into account and may be computed from (1) [4] as:

$$\varepsilon_{re} = \frac{\varepsilon_r \left(1 + g/h\right)}{1 + \left(\varepsilon_r \cdot g/h\right)} \tag{1}$$

where ε_r is the dielectric constant, g the height of the air gap, and h the thickness of the dielectric substrate. The outer ring was chosen slightly larger than the patch dimensions as suggested in [10], and later it was fine tuned to get optimum response.

Table 1. Physical parameters for the proposed antenna geometries.

Geometry parameter		Symbol	Physical dimension (mm)
Length of:	Rectangular patch	L_p	32.2
	Rectangular slot	Ls	22.4
	Ring	L_r	39.0
	Tapered strip	t	1.6
Width of:	Rectangular patch	W_p	39.2
	Rectangular slot	Ws	22.4
	Ring	W_r	41.4
	Tapered strip	s	14
Thickness of ring		T_r	1.0
Tapering of parasitic strip (from top & bottom)		T_p	4.0
Distance between probe & patch (edge to edge)		d	0.4
Air gap		g	4.5
Position of slot from center of rectangular patch		x, y	10.5, 0

3. ANTENNA DESIGN AND ITS OPTIMIZATION

In this section, the design and optimization of the proposed antenna geometry are covered. The parametric analysis was carried out to get the final optimum geometry. The parameters used for the optimization of the antenna are the air gap, the position of the slot, and the position of the tapered strip & probe pin. The optimization of these parameters is covered in the following subsections.

3.1. Air gap Variation

The initial value of the air gap was calculated from (2) [4], and then its values were fine-tuned to arrive at the final value.

$$g \cong 0.16\lambda_c - h\sqrt{\varepsilon_r} \tag{2}$$

where λ_c is the wavelength corresponding to the center frequency of the operating band, h the thickness of the substrate, and ε_r the relative dielectric constant. The air gap was varied in steps of 0.5 mm from the initial value on either side. The effects of variation of the air gap on reflection coefficient parameters and on the gain vs. frequency characteristics are presented in Figure 2. It may be noticed from Figure 2 that for all values of the air gap, a total of six resonances are excited. The only variation observed in the reflection coefficient characteristics is the shift in the 4th band, and the bandwidth reaches maximum for the air gap value of 4.5 mm. Further, it may be noticed from gain vs. frequency curves that a peak gain of 7.39 dBi was obtained for the 3rd resonance (3.03 GHz), and apeak gain value of 5.93 dBi was obtained at the 4th resonant band. Variations in the peak gain due to changes in air gap data are listed in Table 2. The top row of Table 2 indicates the different values of air gap considered in this study, and the first column indicates the six resonances for each of these air gap values. Here also, an optimum air gap value of 4.5 mm was obtained.

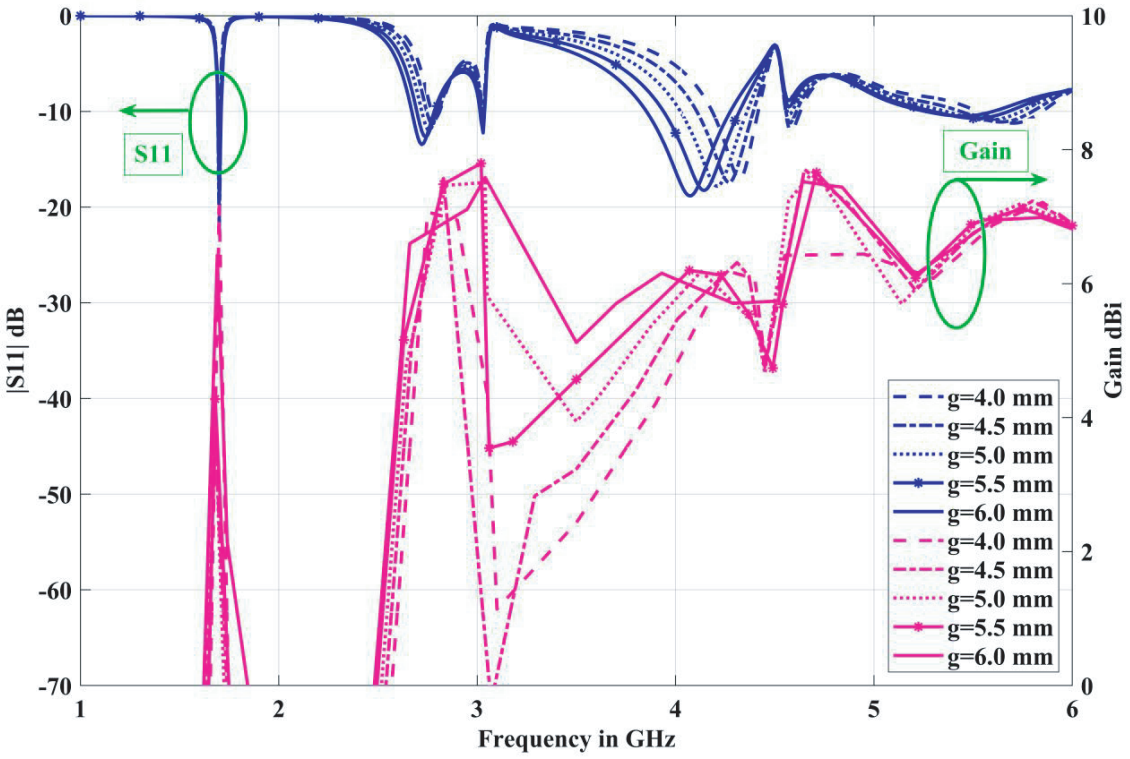

Figure 2. Antenna characteristics variations for different air gap values.

Table 2. Peak gain variations due to change in air gap values.

Air gap (mm)	4.00	4.50	5.00	5.50	6.00
Frequency (GHz)	Peak gain in dBi corresponding to six resonant frequencies				
1.70	7.16	7.29	2.15	3.03	5.57
2.77	7.05	6.10	6.51	6.76	6.79
3.03	4.71	7.39	7.51	6.73	7.53
4.26	6.19	5.93	5.81	6.00	5.74
4.58	6.42	6.22	7.28	6.16	6.63
5.64	6.93	7.03	7.07	7.02	6.96

3.2. Position of Rectangular Slot on the Rectangular Patch

It is well known that adding stubs, slots, etc. excites additional resonances. Hence, in order to excite multiple resonances, the patch element was loaded with a rectangular slot. The dimensions of the slot are optimized as suggested in [9]. The position of the slot is varied from 9 mm to 11 mm (away from the center of the patch), and the corresponding reflection coefficient parameters are depicted in Figure 3. For the slot position of 10.5 mm, the optimum characteristics have been obtained. It may be further noticed that the variation of this parameter does not have much impact on the S_{11} parameters except for the 5th resonance, but there are a lot of fluctuations in the gain of the antenna. Hence, while choosing the optimum values, peak gain values have been taken into consideration (pl. ref. Table 3). In Table 3, the first row indicates the different values of slot positions, and the first column indicates the

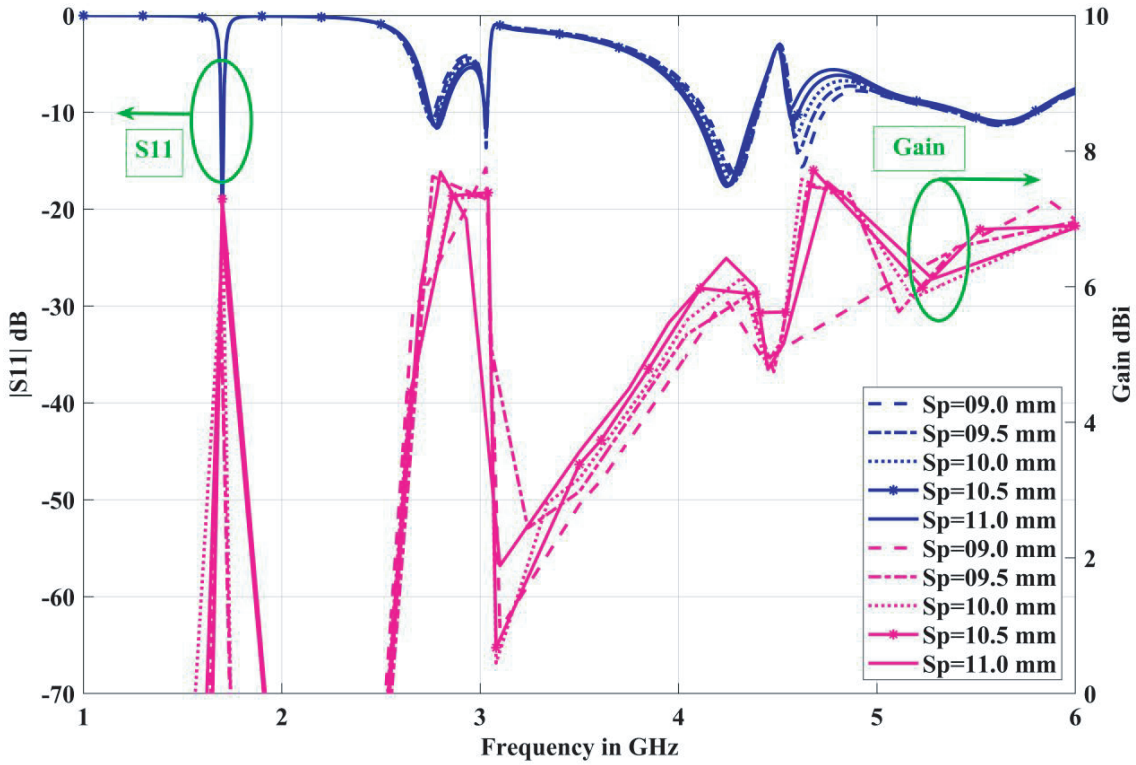

Figure 3. Return-loss characteristics versus frequency for different positions of slot.

Table 3. Peak gain variations due to change in position of rectangular slot from centre of patch.

Slot position (mm)	**9.0**	**9.50**	**10.0**	**10.50**	**11.0**
Frequency (GHz)	**Peak gain in dBi corresponding to six resonant frequencies**				
1.70	4.77	4.84	7.30	7.29	7.29
2.77	6.23	7.61	6.14	6.10	7.19
3.03	7.75	7.29	7.33	7.39	3.99
4.26	5.72	5.70	6.00	5.93	6.36
4.58	5.18	6.24	6.63	6.22	5.70
5.64	6.92	7.11	6.84	7.03	6.93

six resonances obtained for each of these slot position values. From Table 3, it may be noted that the antenna has an optimum performance for the slot position of 10.5 mm (5th column of Table 3).

3.3. Position of Tapered Strip & Probe Pin

The third design parameter is the position of the parasitic tapered strip and the probe pin away from the boundary of the microstrip antenna with slot (rectangular patch geometry). The center of the parasitic strip coincides with the probe pin, but they are not physically connected to each other. This parameter was varied from 17.1 mm to 17.5 mm in steps of 0.1 mm. These effects are shown in Figure 4. In this study, the optimum value of d was found to be 0.4 mm. As mentioned in earlier paragraphs, although there are minor changes in the S_{11} characteristics, here too, notable peak gain variations

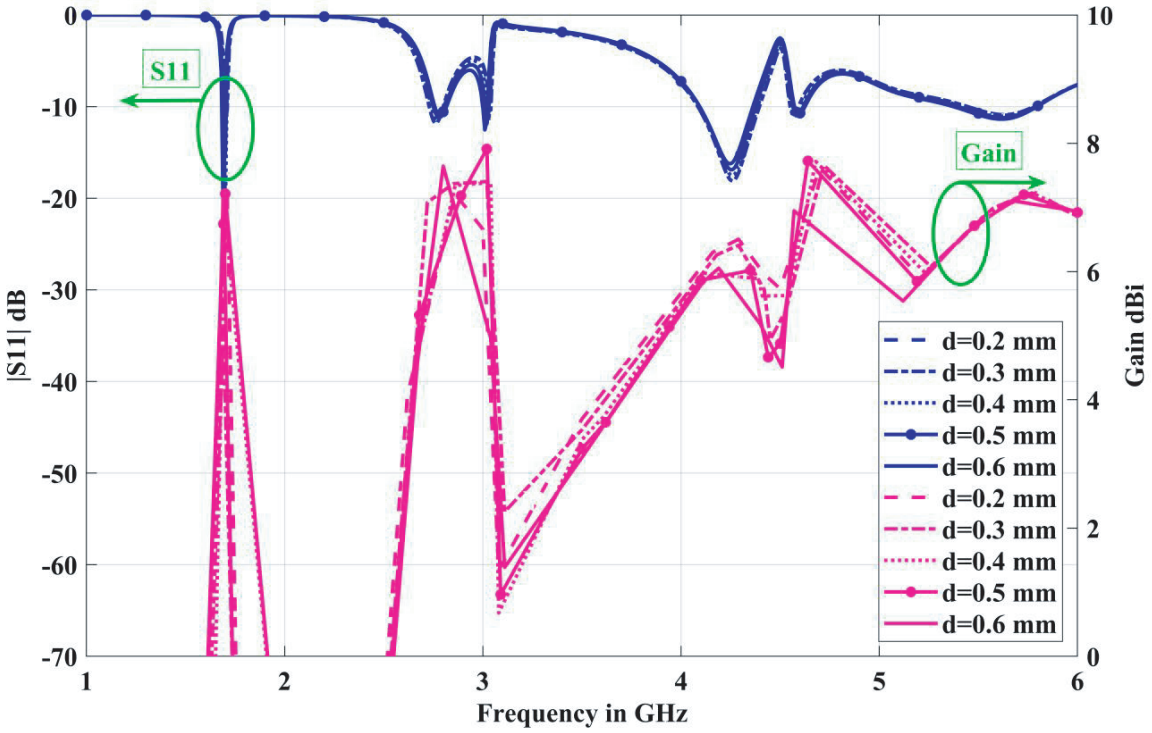

Figure 4. Antenna characteristics variations for different positions of tapered strip.

Table 4. Peak gain variations for different values of distance between feed position and patch.

Strip position (mm)	**0.20**	**0.30**	**0.40**	**0.50**	**0.60**
Frequency (GHz)	**Peak gain in dBi corresponding to six resonant frequencies**				
1.70	6.50	3.96	**7.29**	7.21	5.68
2.77	6.04	7.19	**6.10**	6.12	6.94
3.03	4.67	6.83	**7.39**	6.92	5.06
4.26	6.46	6.37	**5.93**	5.96	5.76
4.58	6.49	6.00	**6.22**	6.50	6.92
5.64	7.07	7.07	**7.03**	7.02	7.04

may be observed. The optimum peak gain values obtained from these investigations are 7.29 dBi, 6.10 dBi, 7.39 dBi, 5.39 dBi, 6.22 dBi, & 7.03 dBi, respectively, corresponding to the six resonances (pl. ref. Table 4). It may be noted that Table 4 shows the performance of the antenna for different values of d (top row), which is the distance between the feed position and the edge of the radiator patch. From this study, it may be noted that for a strip or probe location of 0.4 mm (pl. ref. 4th column of Table 4) away from the main patch's edge, the antenna has optimum performance.

The 3D radiation patterns at all six resonant modes are plotted in Figure 5. From the 3D patterns, it may be noted that at all resonances, radiation characteristics are stable, and the first three resonances have their peaks at bore sight angles. For the last three resonances, the patterns have tilted slightly.

Further, in order to demonstrate the design flexibility, the antenna geometry was scaled up and down from the original geometry's physical dimensions in steps of 5% on either side of the original dimensions, i.e., 0.95, 1.0, and 1.05, keeping the z value $(g + h)$ constant. In this study, it was observed

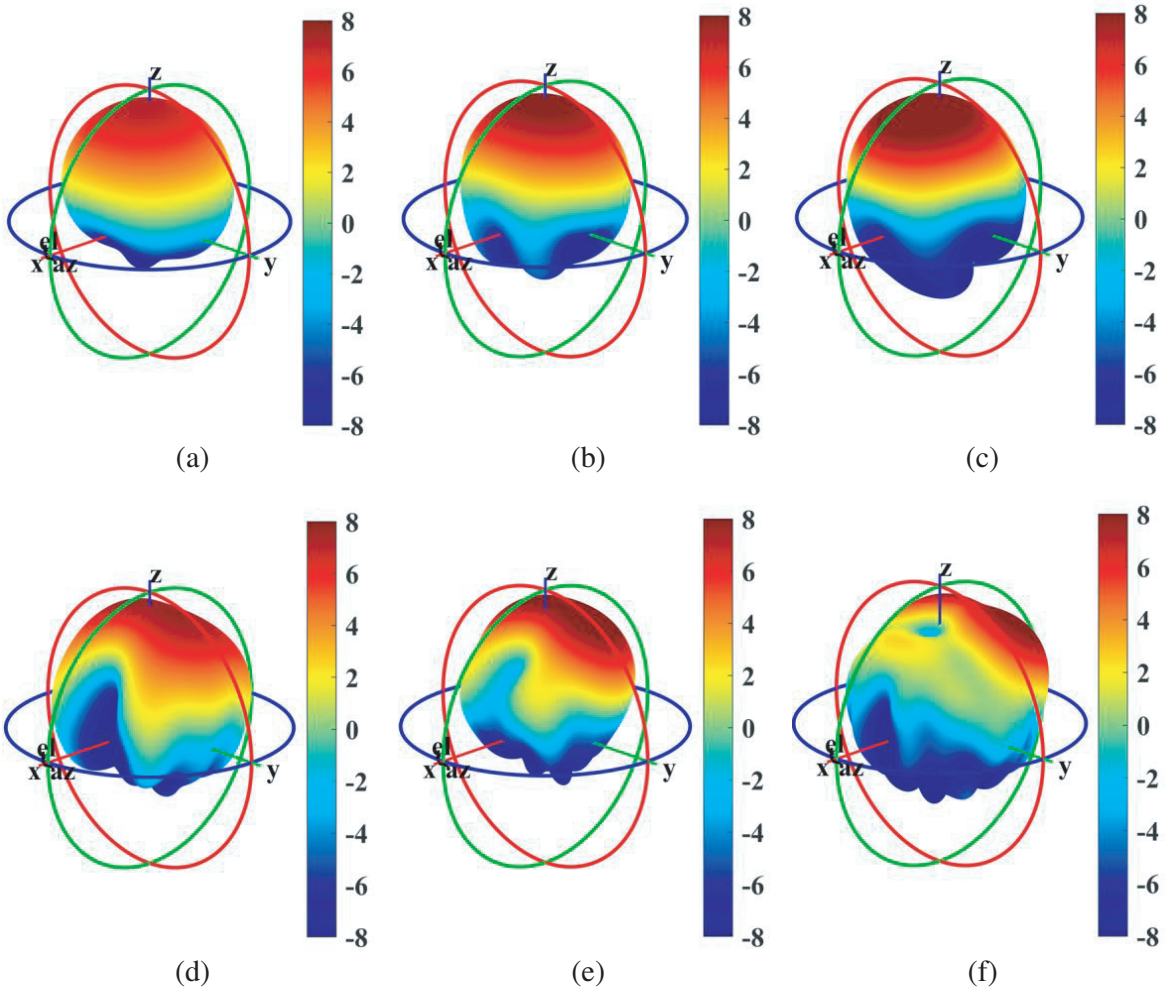

Figure 5. 3D radiation patterns showing the realized gain of the proposed antenna. (a) 1.7 GHz. (b) 2.77 GHz. (c) 3.03 GHz. (d) 4.26 GHz. (e) 4.58 GHz. (f) 5.64 GHz.

that the resonances may be reconfigured to desired operational frequency values. However, the air gap has to be further fine-tuned to obtain the optimum response. The input characteristics of this study are shown in Figure 6. This figure clearly indicates that operational frequencies can be reconfigured or tuned to desired frequencies of operation.

4. EXPERIMENTAL RESULTS & ANALYSIS

The antenna proposed in Section 2 & optimized in Section 3 with dimensions listed in Table 1 was fabricated and tested (measured) with the help of Agilent's N5230A network-analyzer. The antenna substrate used for the study & for the practical realization is a Rogers' RT Duroid 5880 with a dielectric constant of 2.5 and a height of 3.12 mm (obtained from two pieces of 1.56 mm substrate). The S_{11} (measured & simulated) data of the presented geometry are given in Figure 7. From these results, it may be observed that the measured and simulation data match each other fairly. The measured S_{11} curves indicate that the resonances are at 1.7 GHz, 2.73 GHz, 3.03 GHz, 4.165 GHz, 4.56 GHz, and 5.89 GHz. Corresponding gain values are 6.92 dBi, 7.72 dBi, 4.88 dBi, 5.34 dBi, 4.25 dBi, and 6.51 dBi, respectively (Figure 8). The performance parameters of the presented antenna are listed and compared with simulated data in Table 5. The radiation patterns presented here (Figure 9) reveal that co-polarizations values in both principal planes (E- & H-planes) are stable at all operational resonant

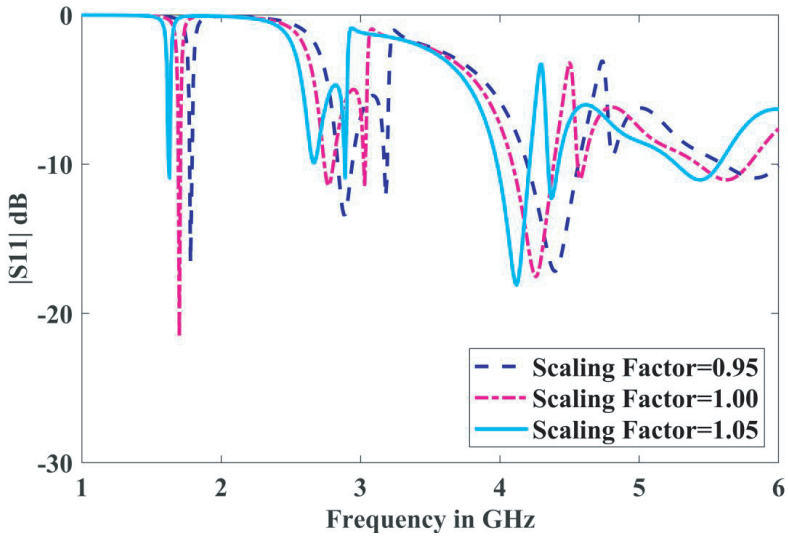

Figure 6. Reflection coefficient characteristics of the proposed antenna for different scaling factors.

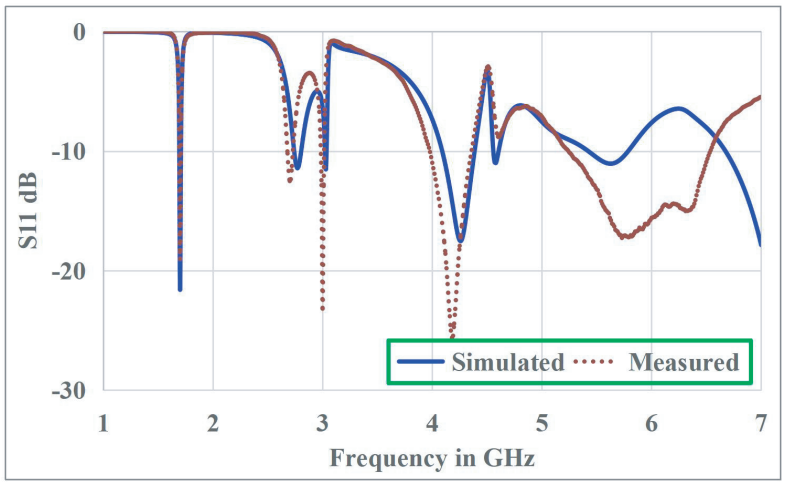

Figure 7. S_{11} parameters comparisons of the antenna presented in Figure 1.

Table 5. Performance parameters of the proposed antenna.

Band No.	Antenna performance comparison (Simulated, Measured)			
	f_1 (MHz)	f_2 (MHz)	BW (MHz) ($S_{11} < -10$ dB)	Peak Gain in dBi
Band 1	1690, 1690	1710, 1710	20, 20	7.29, 6.92
Band 2	2740, 2720	2800, 2740	60, 20	6.10, 7.72
Band 3	3020, 3020	3030, 3030	10, 10	7.39, 4.88
Band 4	4090, 3980	4390, 4350	300, 370	5.93, 5.34
Band 5	4560, 4560	4610, 4560	50, –	6.22, 4.25
Band 6	5420, 5250	5790, 6530	370, 1280	7.03, 6.51

frequencies. In all cases plotted here, the cross-polarization levels are better than −15 dB at bore-sight angles. Results obtained in this work are compared with the contemporary works on multi-band antennas available in literature (listed in Table 6). Further, from this data, it may be concluded that the proposed antenna geometry is simple as well as easy to design and also offers significant results, i.e., six resonances with good gain and good radiation parameters except for slight asymmetry at higher operational frequencies.

Table 6. Comparison of proposed antenna with its contemporary designs available in literature.

Ref. No.	Antenna Dimensions	No. of bands	Center Frequency (GHz)	Peak gain (dBi)	Applications/ Additional remarks
[17]	$30 \times 20 \times 1.6\,\text{mm}^3$	03	2.4/3.3/5.8	1.8/2.5/3.4	Wearable and Tumor Detection
[18]	$80 \times 80 \times 3.175\,\text{mm}^3$	04	1.56/2.49/ 3.5/5.24	3.49/6.49/ 4.93/4.46	GPS, IRNSS, WLAN, Sub-6 GHz 5G
[19]	$100 \times 100 \times 3.175\,\text{mm}^3$	04	1.728/2.127/ 2.358/3.436	6.29/7.08/ 4.51/6.18	2G, 3G, 4G, Sub-6 GHz 5G.
[20]	$50 \times 60 \times 3.0\,\text{mm}^3$	04	0.835/5.59/ 9.52/13.67	−3.1/5.91/ 1.5/10.3	Radio location in UHF, ARNS, C, X, and Ku band applications
[21]	$32 \times 32 \times 1.6\,\text{mm}^3$	05	3.58/5.9/6.72/ 8.51/9.76	1.2/1.6/ 2.1/2.5/2.7	WLAN WiMAX Satellite TV, and X-band
[22]	$35 \times 30 \times 1.6\,\text{mm}^3$	05	1.6/2.3/3.4/ 5.7/10.14	3.9/3.7/1.13/ 2.16/5.36	GPS/GNSS/ Bluetooth/ WiMAX/X-band
[23]	$31 \times 27 \times 1.6\,\text{mm}^3$	06	2.6/3.5/4.2/ 4.5/5.0	1.72/1.94/ 2.51/2.81/ 3.66/3.8	Sub-6 GHz 5G; 8 switches; Multibeam
[25]	$30 \times 30 \times 1.6\,\text{mm}^3$	07	0.77/1.43/ 2.13/3.48/ 3.84/5.17/6.0	1.1/1.3/ 1.1/1.6/ 1.7/1.8/2.2	WLAN, WiMAX, Sub-6-GHz 5G, Medical telemetry, DBC (Digital Broadcasting)
[This Work]	$\mathbf{41.4 \times 39 \times 3.12\,mm^3}$	**06**	**1.70/2.77/ 3.03/4.26/ 4.58/5.64**	**7.29/6.10/ 7.39/5.39/ 6.22/7.03**	**LTE, WLAN, Amateur Radio, Sub 6 GHz 5G**

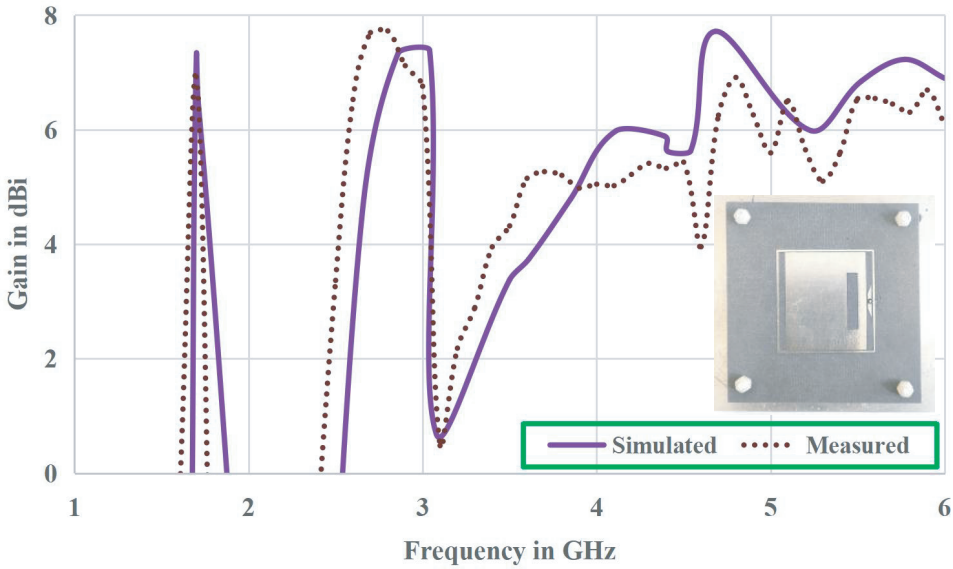

Figure 8. Gain characteristics comparisons of the proposed antenna.

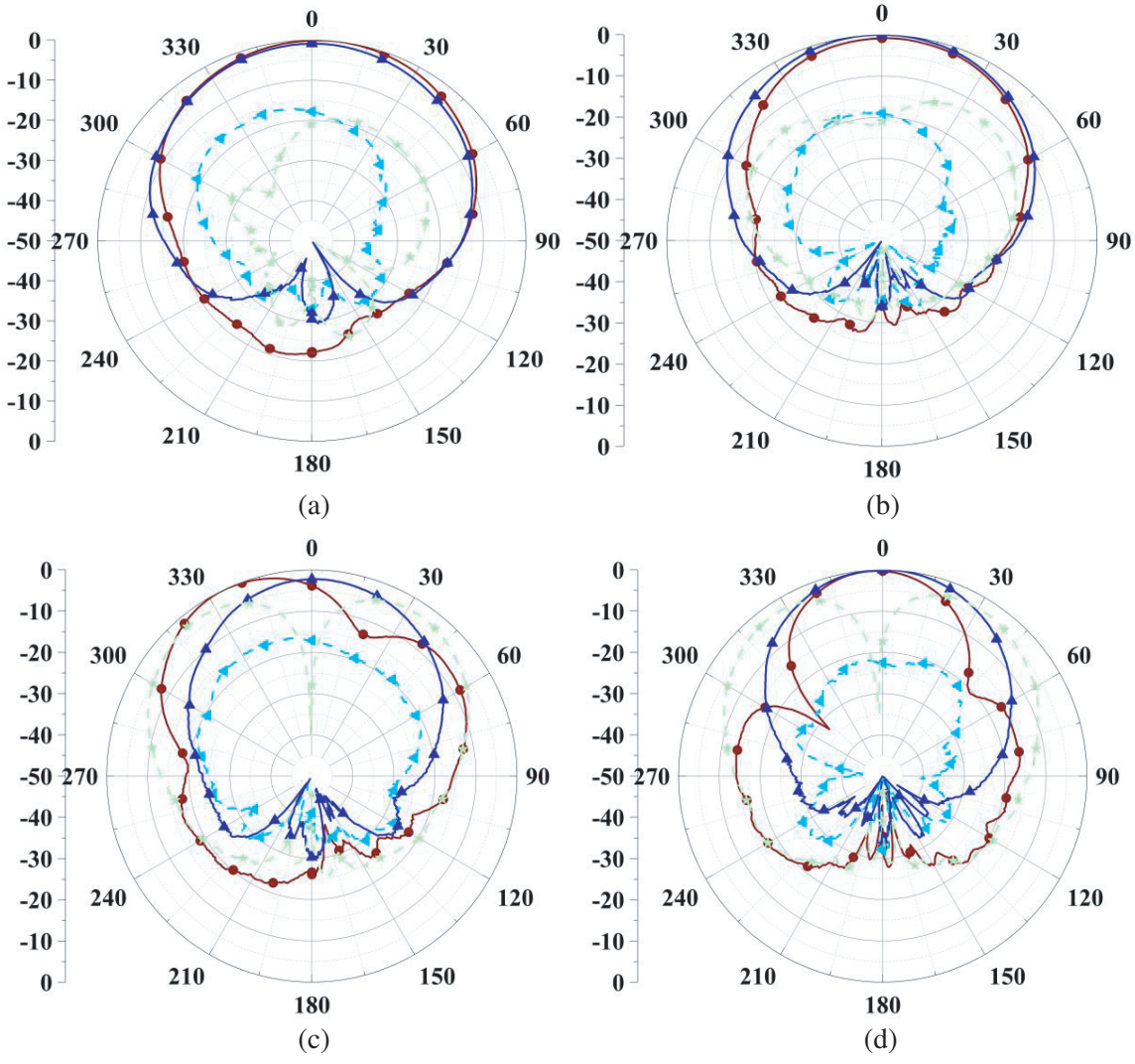

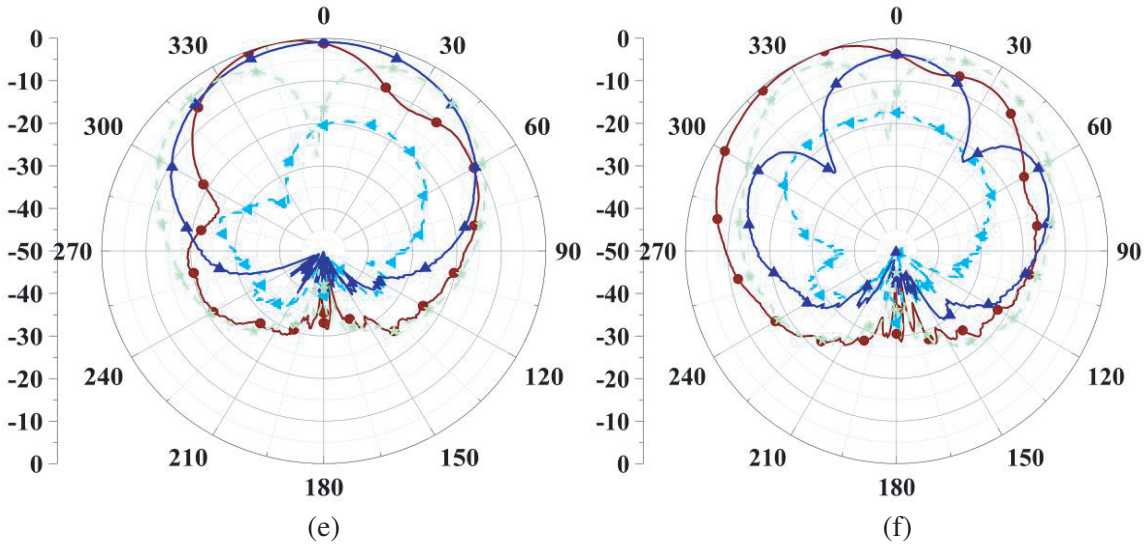

Figure 9. Measured radiation data at six resonances (E plane co-polarization: solid brown; H plane co-polarization: solid blue; E plane cross-polarization: dashed green; H plane cross polarization: dashed cyan). (a) 1.70 GHz. (b) 2.77 GHz. (c) 3.03 GHz. (d) 4.26 GHz. (e) 4.58 GHz. (f) 5.64 GHz.

5. CONCLUSIONS

A gap coupled high gain multiband microstrip antenna suitable for LTE, WLAN, mature radio, and sub-6 GHz 5G wireless applications has been presented. A gap-coupled probe feed along with a tapered parasitic strip was used to tune the antenna's input impedance. An additional ring and a slot loaded on the patch have been used to excite multiple resonances. The presented antenna offers a total of six resonant frequencies centered at 1.70 GHz, 2.77 GHz, 3.03 GHz, 4.26 GHz, 4.58 GHz, and 5.64 GHz, with corresponding gain values at the frequencies of 7.29 dBi, 6.10 dBi, 7.39 dBi, 5.39 dBi, 6.22 dBi, and 7.03 dBi, respectively. A good match between the measured and simulated data was observed. The proposed antenna exhibits a very good gain, as high as 7.72 dBi. Nearly stable radiation parameters have been obtained at all operational frequencies.

ACKNOWLEDGMENT

The authors would like to thank the ECE Department's Chairman, Prof. K. J. Vinoy and his research scholar, Mr. Gaurang of the Indian Institute of Science, Bangalore, for providing measurement laboratory facilities. The authors also acknowledge the Department of Science and Technology of the Karnataka Govt. for approving the first author's research fellowship. The authors further acknowledge Dr. R. Joshi, Associate Professor in the department of Physics at C. U. Karnataka, for allowing them to use the microwave measuring lab.

REFERENCES

1. Yin, J., Q. Wu, C. Yu, H. Wang, and W. Hong, "Broadband symmetrical E-shaped patch antenna with multi-mode resonance for 5G millimeter-wave applications," *IEEE Transactions on Antennas and Propagation*, Vol. 67, No. 7, 4474–4483, July 2019.
2. Lu, H., F. Liu, W. Wang, Z. Gao, X. Bai, and Y. Liy, "Capacitive probe compensation-fed wideband patch antenna with U-shaped parasitic elements for 5G/WLAN/Wi-Max applications," *IEICE Express*, Vol. 16, No. 16, 1–6, 2019.

3. Singh, D. K., B. K. Kanujia, S. Dwari, and G. P. Pandey, "Modeling of a dual circularly polarized capacitive-coupled slit loaded truncated microstrip antenna," *Journal of Computational Electronics*, Vol. 19, No. 4, 1564–1572, 2020.
4. Kasabegoudar, V. G. and K. J. Vinoy, "Coplanar capacitively coupled probe fed microstrip antennas for wideband applications," *IEEE Transactions on Antennas and Propagation*, Vol. 58, No. 10, 3131–3138, 2010.
5. Kasabegoudar, V. G. and P. Reddy, "A review of low profile single layer microstrip antennas," *International Journal of Electrical and Electronic Engineering & Telecommunications*, Vol. 11, No. 2, 122–131, 2022.
6. Reddy, P. and V. G. Kasabegoudar, "Gap coupled suspended ultra-wideband microstrip antennas for 5G applications," *International Journal of Engineering Trends and Technology*, Vol. 71, No. 2, 371–381, 2023.
7. Sun, W., Y. Li, L. Chang, H. Li, X. Qin, and H. Wang, "Dual-band dual-polarized microstrip antenna array using double-layer gridded patches for 5G millimeter-wave applications," *IEEE Transactions on Antennas and Propagation*, Vol. 69, No. 10, 6489–6499, October 2021.
8. Yang, S., G.-M. Zhang, X.-D. Yue, J.-L. Ru, and G.-P. Fan, "A dual-frequency broadband patch antenna with L-shaped probe feed for 5G communication," *2019 International Symposium on Antennas and Propagation (ISAP)*, 1–3, 2019.
9. Kasabegoudar, V. G., "Dual frequency ring antennas with coplanar capacitive feed," *Progress In Electromagnetic Research C*, Vol. 23, 27–39, 2011.
10. Kasabegoudar, V. G. and A. Kumar, "Dual band coplanar capacitive coupled microstrip antennas with and without air gap for wireless applications," *Progress In Electromagnetic Research C*, Vol. 36, 105–117, 2013.
11. Mok, W. C., S. H. Wong, K. M. Luk, and K. F. Lee, "Single-layer single-patch dual-band and triple-band patch antennas," *IEEE Transactions on Antennas and Propagation*, Vol. 61, No. 8, 4341–4344, 2013.
12. Gao, M. and X. Zhao, "Design of tri-band patch antenna with enhanced bandwidth and diversity pattern for indoor wireless communication," *Applied Sciences*, Vol. 12, 1–13, 2022.
13. Elkorany, A. S., et al., "Implementation of a miniaturized planar tri-band microstrip patch antenna for wireless sensors in mobile applications," *Sensors*, Vol. 22, 2022.
14. Wang, L., J. Yu, T. Xie, and K. Bi, "A novel multiband fractal antenna for wireless application," *International Journal of Antennas and Propagation*, 1–9, 2021.
15. Rengasamy, R., D. Dhanasekaran, C. Chakraborty, and S. Ponnan, "Modified Minkowski fractal multiband antenna with circular-shaped split-ring resonator for wireless applications," *Measurement*, Vol. 182, 1–9, 2021.
16. Khan, Z., et al., "A single-fed multiband antenna for WLAN and 5G applications," *Sensors*, Vol. 20, 1–13, 2020.
17. Sharma, N., A. Kumar, A. De, and R. K. Jain, "Design of compact hexagonal shaped multiband antenna for wearable and tumor detection applications," *Progress In Electromagnetic Research M*, Vol. 105, 205–217, 2021.
18. Patel, D. H. and G. D. Makwana, "Multiband antenna for GPS, IRNSS, sub 6 GHz 5G and WLAN applications," *Progress In Electromagnetic Research M*, Vol. 116, 53–63, 2023.
19. Patel, D. H. and G. D. Makwana, "Multiband antenna for 2G/3G/4G and sub-6 GHz 5G applications using characteristic mode analysis," *Progress In Electromagnetic Research M*, Vol. 115, 107–117, 2023.
20. Kumar, A. and A. P. S. Pharwaha, "Development of a modified Hilbert curve fractal antenna for multiband applications," *IETE Journal of Research*, 1–10, 2020.
21. Ali, T., K. D. Prasad, and R. C. Biradar, "A miniaturized slotted multiband antenna for wireless applications," *Journal of Computational Electronics*, Vol. 17, 1056–1070, 2018.

22. Ali, T., F. Nikhat, and R. C. Biradar, "A miniaturized multiband reconfigurable fractal slot antenna for GPS/GNSS/Bluetooth/WiMAX/X-band applications," *AEU — International Journal of Electronics and Communication*, Vol. 94, 234–243, 2018.
23. Ahmad, I., et al., "Design and experimental analysis of multiband compound reconfigurable 5G antenna for sub-6 GHz wireless applications," *Wireless Communications and Mobile Computing*, 1–14, 2021.
24. Sultan, K., M. Ikram, and N. Nguyen-Trong, "A multiband multibeam antenna for Sub-6 GHz and mm-wave 5G applications," *IEEE Antennas and Wireless Propagation Letters*, Vol. 21, No. 6, 2022.
25. Desai, A., et al., "Multiband inverted E and U shaped compact antenna for digital broadcasting, wireless, and sub 6 GHz 5G applications," *International Journal of Electronics and Communication*, Vol. 123, 1–8, 2020.